Molecular changes in fibrillar collagen in myxomatous mitral valve disease

ELSEVIER

Cardiovascular Pathology 19 (2010) e141 – e148

CARDIOVASCULAR PATHOLOGY

Original Article

Molecular changes in fibrillar collagen in myxomatous mitral valve disease

Mojtaba Hadian[a,*], Brendan M. Corcoran[b], Jeremy P. Bradshaw[a]

[a]*Veterinary Biomedical Sciences, Royal (Dick) School of Veterinary Studies, University of Edinburgh, Summerhall, EH9 1QH Edinburgh, UK*
[b]*Hospital for Small Animals, Veterinary Clinical Sciences, Easter Bush Veterinary Centre, Royal (Dick) School of Veterinary Studies, University of Edinburgh, EH25 9RG Roslin Midlothian, UK*

Received 4 November 2008; received in revised form 24 April 2009; accepted 19 May 2009

Abstract

Introduction: Myxomatous mitral valve disease (MMVD) is the single most common acquired cardiac disease of dogs and is a disease of significant veterinary importance. It also bears close similarities to mitral valve prolapse in humans and therefore is a disease of emerging comparative interest. We have previously mapped the structure of collagen fibrils in valve leaflets using synchrotron X-rays and have demonstrated changes in collagen structure associated with the regions of disease. **Methods:** Differential scanning calorimetry (DSC), biochemical assay of collagen content, high-performance liquid chromatography (HPLC), and neutron diffraction were combined with further analysis of our previous X-ray data to elucidate molecular changes in fibrillar collagen in mild to moderately affected MMVD dogs. **Results:** Comparing diseases and adjacent grossly uninvolved areas in the same leaflets, there was a 20% reduction in collagen fibrils, but only a 10% depletion of collagen content. The enthalpy of collagen denaturation was reduced in affected areas. Chromatography showed a 25% decrease in mature nonreducible covalent cross-links in the affected samples, and neutron diffraction data showed fewer reducible immature covalent cross-links in grossly uninvolved tissue samples. **Conclusions:** Mild to moderate MMVD in the dog is associated with a marginal decline in collagen content in overtly diseased areas of valves, but more importantly is associated with an increase in immature collagen content. These changes will contribute to the mechanical dysfunction of the leaflet, and this study provides important information on the structure–mechanical alterations associated with this disease. The data suggests MMVD involves a dyscollagenesis process in the development of valve pathology.

Keywords: Myxomatous mitral valve (MMV); Differential scanning calorimetry (DSC); Neutron diffraction; High-performance liquid chromatography (HPLC); Collagen; Dog

1. Introduction

Myxomatous mitral valve disease (MMVD) is the single most common acquired cardiac disease of dogs and is a disease of significant veterinary importance. It has a close breed and age association, such that certain breeds are overrepresented and all middle-to old-aged dogs will have varying degrees of disease [1,2]. It is also of comparative interest in that it bears close similarity to mitral valve prolapse in humans [3]. This disease is of increasing importance in the ageing human population and involves major research activity in the areas of novel surgical techniques and tissue engineering of prosthetic replacement valves. The condition, in both dogs and humans, is typified by the loss of mechanical integrity of the valve leaflets, failure of proper coaptation of the leaflet edges during ventricular systole, and mitral valve regurgitation. This loss of mechanical integrity is a consequence of the destruction of the fibrosa layer, expansion of the loose connective tissue spongiosa layer, and excessive accumulation of glycosaminoglycans [2,4–6]. However, there are conflicting data on the exact role of collagen depletion or alteration in this disease in both dogs and humans [4,6–8]. Collagen abnormalities have been identified in affected dogs on

The work was supported by the Institute Laue Langevin (Grenoble, France), the Kennel Club Charitable Trust, and the Cavalier King Charles Spaniel Club of England. Mojtaba Hadian is sponsored by Iran Ministry of Science.

* Corresponding author. Veterinary Biomedical Sciences, Royal (Dick) School of Veterinary Studies, University of Edinburgh, Summerhall, EH9 1QH Edinburgh, UK. Tel.: +44 0 1316506142; fax: +44 0 131 650 6511.
E-mail address: m.hadian@ed.ac.uk (M. Hadian).

1054-8807/09/$ – see front matter
doi:10.1016/j.carpath.2009.05.001

transmission electron microscopy, and we have previously shown altered collagen distribution using X-ray diffraction [9,10]. This and other data support the idea that MMVD is a dyscollagenesis disorder and is associated with valve interstitial cell phenotypic transformation and migration in both dogs and humans [11–14]. The valve interstitial cells are responsible for extracellular matrix production, and those alterations in the ECM, including changes in collagen organization, are presumed to contribute to the mechanical instability of affected valves [2,9,10,13].

We are interested in investigating changes in fibrillar collagen in MMVD. All the fibril-forming collagens, including Types I, II, III, V, and IV, have a triple-helical structure which contains approximately 1000 amino acids measuring 300 nm in length. Collagen is synthesized as the precursor procollagen containing non-triple-helical amino- (N) and carboxylic-terminal (C) extensions. Formation of fibrils requires an initial linear and lateral aggregation that is promoted by the presence of these two propeptide extensions, but also physically limited by their presence. The removal of the N-propeptide and C-propeptide allows closer lateral assembly. The resulting structure displays the classic microscopic features of tissue collagen fibrils. Prior to maturation, electrostatic forces, hydrogen bonds, and hydrophobic interactions are mainly responsible for holding these molecules together. However, as fibrils mature, they develop from a highly soluble material to an insoluble and inert structure. This transformation is largely attributed to the formation of strong inter- and intramolecular cross-links, and these cross-links are vital for providing collagen matrices with stability and tensile strength. The type and degree of cross-linking vary between different tissues and are affected by a variety of factors, including the degree of posttranslational modification and molecular packing [15,16]. In the absence of cross-links, the molecules are capable of sliding against each other resulting in a very weak and extensible fiber, for example, as found in some forms of osteogenesis imperfecta [17].

We have previous shown alteration in collagen distribution in canine MMVD [10], and the current study was designed to investigate collagen content and the nature of cross-linking, including mature and immature forms, in the collagen fibrils of valve leaflets affected by MMVD. This involved measurement of the thermal properties of the collagen using differential scanning calorimetry (DSC), quantitative assay of collagen content using a hydroxyproline assay, and investigation of cross-links using neutron diffraction and high-performance liquid chromatography (HPLC).

2. Materials and methods

2.1. Animals

Mitral valve leaflets were obtained from middle-aged dogs (average age approximately 7 years) presented to the Hospital for Small Animals, the University of Edinburgh for euthanasia. All procedures and sampling were carried out with full owner consent. Mitral valve complexes were obtained within 10 min of death, gently washed with phosphate-buffered saline (PBS), and immediately snap frozen in dry ice using OTC as cryoprotectant and stored at −60°C until required. At the time of collection, the extent of valve pathology was assessed by two experienced veterinary cardiologists and attributed a gross pathological grade according to the method of Whitney [18]. Briefly, this classification grades valve leaflet 1 to 4, with Grade 4 indicating severe pathological change. All leaflets in this study graded between 1 and 2, indicating moderate disease, where visibly diseased areas coexisted adjacent to areas of grossly uninvolved valve tissue. This also gave us the opportunity of comparing the affected areas with healthy ones in the same valve leaflet, since the opportunity to identify age-matched normal valves in the pet dog population is extremely difficult. Since MMVD equally affects the anterior (septal) and posterior (mural) leaflet in the dog, the tissue from both leaflets was pooled for sampling [12].

Prior to each experiment, the samples were allowed to thaw at room temperature and then were again gently cleaned with PBS. Diseased and the adjacent grossly uninvolved areas from different leaflets were identified and carefully excised. Since type I collagen is the main constituent of tendons (>95%) [19], dog and rat tail tendon were also obtained for comparison. All reagents and chemicals were supplied by Sigma-Aldrich unless specified otherwise.

2.2. Differential scanning calorimetry

Tissue samples were chosen and excised from the affected and the adjacent grossly uninvolved areas of the valve leaflets, as described above. They were blotted with a soft tissue. After weighing the samples, calorimetric measurements were performed using a Perkin-Elmer Pyris 1 differential scanning calorimeter. Heating was carried out from 10°C to 80°C at a rate of 5°C/min, after initial holding at 10°C for 2 min. An empty pan was used as a reference. The onset temperature and enthalpy (ΔH) were calculated from thermograms for each process. The enthalpy was determined from the area between extrapolated peak onset and extrapolated peak completion. In total, for the purpose of the DSC experiment, 10 diseased and seven unaffected samples (from four different leaflets obtained from dogs) were examined. Dog and rat tail tendons were also run for comparison and to ensure reproducibility of the data. After completion of the measurements, the sample pans were punctured and placed under vacuum for 3 h to desiccate before they were reweighed. The instrument was calibrated with indium and water as standards.

2.3. Hydroxyproline assay

An adapted form of the Bergman and Loxley method was used to determine the hydroxyproline content of mitral

valves [20]. Since hydroxyproline is exclusively found in collagen, where it comprises 13.4% of the protein, the total concentration of collagen can be determined by multiplying the hydroxyproline value by 7.46. Mitral valve leaflets (three diseased and three healthy from different dogs) were selected and cut to produce 3×3-mm samples, and their wet weight measured. Additional samples were prepared from dog tail tendon. The tissues were dehydrated in 1 ml acetone (60 min) and degreased in 2 ml petroleum ether (120 min). The fragments were dried in an incubator at 100°C for 30 min. Drying continued in a freeze-dryer for 6 h. The samples were reweighted again (dry weight). One hundred microliters of 6N HCl was added to each test tube and they were sealed under vacuum. The sealed tubes were incubated at 110°C for 12 h. The hydrolysates were then dried, resuspended in 1 ml HCl (1 mM), and transferred into 1.5-ml Eppendorf tubes. They were centrifuged at 10,000 rpm for 15 min. The supernatants were used for the next step of the experiment. This preparation was carried out in triplicate for each sample. To 100 μl of supernatant in each test tube, the following reagents were added in order: 400 μl HCl (1 mM); 1 ml isopropanol; and 500 μl of an oxidant solution. The antioxidant solution contained 1 ml of 7% chloramine T made in distilled water added to 4 ml of acetate/citrate buffer, pH 6 (14.3 mg sodium acetate trihydrate, 9.4 g trisodium citrate dihydrate, and 1.4 g citric acid monohydrate were dissolved in 96 ml isopropanol and made up to 250 ml with distilled water). Standard hydroxyproline solutions of 1.5, 1, 1/2, 1/4, 1/8, 1/16, 1/32, 1/64, and 1/128 mg/ml were made from L-4-hydroxyproline (Fluka Biochemika) and treated in the same way. A blank control was made by adding 500 μl 1 mM HCl instead of the supernatant or standard solution. The tubes were vortexed and left at room temperature for 4 min. Five hundred microliters of freshly prepared Ehrlish's reagent solution, containing 3 ml of Ehrlish's reagent (10 g paradimethylaminobenzaldehyde in 11 ml 70% perchloric acid) mixed with 16 ml isopropanol, was added to all tubes. The tubes were vortexed again and incubated in a water bath at 37°C for 2 h. The absorbance was read at 550 nm (Varian Cary 50 Scan spectrophotometer) for all the samples, and the concentration of hydroxyproline was calculated against the standard graph.

2.4. Neutron diffraction

The ability of sodium borohydride ($NaBH_4$) to react and reduce the keto-amine and Schiff base groups of mostly aldehyde-based cross-links has been reported previously [15]. The introduction of deuterons into an ordered structure will alter the neutron scattering density profile and therefore its diffraction pattern. Sodium borodeuteride (NaB^2H_4, 98 atom % D) was used to target the reducible cross-links specifically, using the method of Wess et al. [21].The reducing solution was made by dissolving 70 mg of sodium borodeuteride to 5 ml PBS at pH 7.5. Each fresh sample (approx. 1 g in weight) was immersed separately for 20 min followed by washing with PBS at pH 7.4 to stop the reaction.

The instrument D22 at the Institut Laue-Langevin (Grenoble, France) was used to collect small angle scattering data with 7 Å wavelength neutrons. The 96×96-cm detector was placed at two positions, 2.5 and 11.2 m, to collect data spanning the range from the first to the seventh order of meridional diffraction. Neutron scattering data were collected from each mitral valve leaflet sample at each detector position, and then the same samples were treated with sodium borodeuteride and remeasured. Due to constraints on the allocated instrument time, it was only possible to run three samples (one affected and one diseased mitral valve from different dogs and one dog tail tendon from another dog). An empty cell and detector-calibration (water cell) measurements were also performed, for use in correcting and analyzing the data. The *LAMP* program (Large Array Manipulation Program, Institut Laue-Langevin) was used to normalize the data to water with all corrections (transmissions and background) carried out on radially averaged data. Diffraction spectra were obtained by sector summation, and ratios of diffracted intensity were calculated for each of the seven orders of meridional diffraction by dividing the diffracted intensity of treated tissue by the corresponding intensity of untreated tissue. The data sets have been scaled to give a first-order ratio of 1.0. For comparison, equivalent data from an earlier study of rat tail tendon, by Wess et al. [22], were analyzed in the same manner.

2.5. High-performance liquid chromatography

Acetonitrile (HPLC gradient grade), methanol (chromasolve), sodium dihydrogen orthophosphate (NaH2PO4), boric acid, and *o*-phthalaldehyde (OPA-complete solution) were used in this experiment and purchased from Sigma-Aldrich. The mature standard cross-links, pyridinoline (PYD), and deoxypyridinoline (DPD) were kindly supplied by the Rowett Research Institute (Aberdeen, UK). Standard single amino acid collection was from VWR. Chromatography condition was mostly in accordance with the Bartolomeo and Maisano [23] methods. Chromatography was performed on a Pharmacia LKB.VWM 2141 HPLC system at room temperature using Phenomenex Luna 5 μm

Table 1
Gradient used in HPLC

Time (min)	% B
0	0
1.9	0
16.3	100
16.4	100
20	100
21	0
26	0
30	0

Mobile phases were NaH2PO4 40 mM adjusted to pH 7.8 with 2 M NaOH (Buffer A) and acetonitrile/methanol/water (45:45:10) (Buffer B).

C18 (2), reverse-phase column (150×4.6 mm) with UV detection at λ=338 nm. Mobile phases were NaH2PO4 40 mM adjusted to pH 7.8 with 2 M NaOH (Buffer A) and acetonitrile/methanol/water (45:45:10) (Buffer B). Table 1 shows the gradient that was followed for the runs at 2 ml/min.

2.5.1. Precolumn derivatization

The reaction of OPA with primary amines is the result of the formation of an OPA2/2-mercaptoethanol adduct which then reacts with the primary amine of the amino acid to form a highly fluorescent and UV absorbent thio-substitute isoindoles. However, some amino acids cannot be detected by OPA. Proline possesses a secondary amine group and is unable to react with OPA, and the reaction with cysteine also leads to a low response [24]. The reaction is rapid and proceeds at room temperature.

To establish the least sufficient and appropriate concentration ratio of OPA with the given sample in terms of standard amino acids and standard mature cross-links, a total of approximately 100 runs of HPLC were performed. The following approach proved to work best under our laboratory conditions. Regarding the detection of a single primary amino acid, mixing 7.5 nM of OPA with 1 nM of a given amino acid in 0.4 M borate (pH=10.4) and 0.1 M sodium acetate (pH=7.2) and incubation for 1 min at room temperature before injection produced the best results.

A series of runs demonstrated that, at the ratio of 37.5 nM of OPA to 1 nM of DPD or PYD, there was an optimum reaction (Fig. 1). The increased amount of OPA might be explained by the fact that the molecules of the cross-links contain three primary amine groups. Nonetheless, this increase is not proportional when it is compared with the molar concentration of OPA used for determining standard profile single amino acids.

2.5.2. Collagen extraction

Rat tail was frozen immediately after removal from donor rats. During processing, samples were placed in a Petri dish containing 70% ethanol for 20 min. The tip of the tail was cut crosswise with scissors. The skin was pulled back 1/4 in. to expose the tendons, and then each tendon was pulled out with blunt tip forceps. After that, the samples were washed with PBS buffer and cut into pieces (approx. 5×5 mm). Freshly frozen mitral valves were let thaw at room temperature, and then the same procedure was repeated with the only difference that, after cutting them into pieces, they were homogenized. In total, four diseased and four healthy collagen samples were obtained from two diseased and two healthy valve leaflets (Grade 1–2). Collagen was isolated from the rat tail tendons and mitral leaflet samples using previously described methods [25] by dissolving in 0.017 M acetic acid at 4 g/l. The solution was mildly agitated by stirring for 48 h at 4°C. In order to purify the collagen solution, the samples were centrifuged at high speed (10,000×*g*) at 4°C for 1 h in a fixed-angle rotor (JA-20; Beckman Coulter) using a Beckman Coulter high-speed centrifuge [26]. Supernatants were separated and dried using a lyophilizer at −40°C for 12 h. They were weighed into 5-mg groups and hydrolyzed in 200 µl of 6N HCl under vacuum for 12 h. The hydrolysates were dried and resuspended in 700 µl 1 mM HCl and centrifuged at 15,000 rpm for 15 min. Supernatants were filtered and used for HPLC purposes. Then all samples, including the ones obtained from rat tail tendon, were prepared in duplicates.

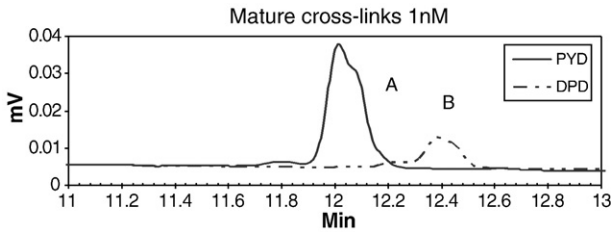

Fig. 1. A typical chromatogram of mature standard cross-links at 1 nM concentration each: pyridinoline (A) and deoxypyridinoline (B).

Table 2
Comparison of thermal parameters for collagen denaturation in dog tail tendon, healthy (grossly uninvolved) dog mitral valve leaflets, and valve leaflets from dogs affected by MMVD

	Onset temperature	Peak temperature	Enthalpy (ΔH)
Dog tail	64.56°C±0.23	65.75°C	8.52 J/g±0.19
Healthy leaflets	65.10°C±0.35	66.37°C	1.75 J/g±0.07
Affected leaflets	64.60°C±0.30	65.45°C	1.40 J/g±0.05

Data are shown as mean values. Measurements were performed on a Perkin-Elmer Pyris 1 differential scanning calorimeter.

3. Results

3.1. Differential scanning calorimetry

Table 2 shows the thermometric parameters determined by DSC for samples of myxomatous and healthy leaflets and

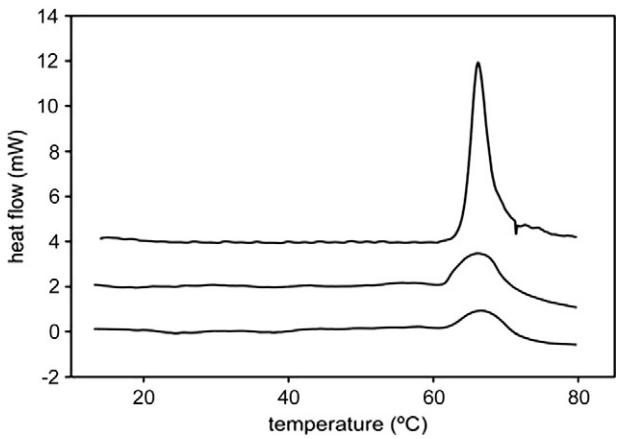

Fig. 2. An example of a DSC thermogram. From top to bottom: dog tail tendon, diseased, and healthy (grossly uninvolved) valve leaflets. The weights of the samples used were as follows: dog tendon 35.2 mg; healthy valve 36.0 mg; diseased valve 36.2 mg.

Table 3
Collagen content of dog tail tendon, healthy (grossly uninvolved) dog mitral valve leaflets, and valve leaflets from dogs affected by MMVD, determined by quantitative analysis of hydroxyproline using an adapted form of the Bergman and Loxley method [20]

	Dried tissue (μg/mg)	Wet tissue (μg/mg)
Healthy	416.15	37.48
Affected	370.06	33.15
Tail tendon	467.17	172.15

dog tail tendon. The data reveal a reduction in enthalpy of denaturation in affected regions of leaflets compared to that of the adjacent grossly uninvolved areas ($P \leq .05$). The onset temperature of the main endothermic peak was slightly lower in affected areas compared to the adjacent grossly uninvolved tissue, but this was not statistically significant. Comparing the leaflets with dog tail tendon (Fig. 2), we found a noticeable difference in enthalpy denaturation for both diseased and the adjacent grossly uninvolved tissues. However, the endothermic peak in tail samples was at the same temperature position as those of the leaflets.

3.2. Hydroxyproline assay

The assay of collagen on the basis of hydroxyproline measurement is summarized in Table 3. Comparison of the data for either dried or wet tissue showed that the quantity of collagen diminished approximately 10% in the affected tissue compared to the adjacent grossly uninvolved tissue. The dried tissue had also been degreased, so the observed difference in collagen content between the dried and wet tissue suggests much higher lipid content in mitral valve tissue compared to tail tendon.

3.3. Neutron diffraction

Table 4 shows the effect of NaB^2H_4 treatment on the three different types of tissue. The results are expressed as ratios of Bragg peak intensity, before and after reduction of the cross-links. There were clear differences in the pattern of altered intensities between tail tendon and healthy heart valve tissue. The intensity changes are larger in tail tendon, suggesting that all mitral leaflets, irrespective of their pathological status (healthy or diseased), have only a small number of reducible cross-links. However, there are also clear differences between the healthy and diseased valves, with the pattern of diseased valves more resembling that of dog tail tendon, implying an increase in the amount of reducible cross-links in the leaflets affected by MMVD.

Table 4
The effect of sodium borodeuteride treatment on the meridional diffraction pattern of collagen from dog tail tendon, healthy (grossly uninvolved) dog mitral valve leaflets, and valve leaflets from dogs affected by MMVD

Diffraction order	Dog tail tendon	Healthy leaflets	Diseased leaflets	Rat tail tendon
1	1.00	1.00	1.00	1.00
2	1.05	0.94	0.94	0.90
3	0.95	0.91	0.93	0.93
4	1.14	0.96	0.99	0.80
5	1.22	1.01	1.01	1.15
6	1.27	1.01	1.03	1.37
7	1.31	0.98	1.05	2.16

The data were calculated by dividing the diffracted intensity of treated tissue by the corresponding intensity of untreated tissue. The data sets have been scaled to give a first-order ratio of 1.0. Also shown are corresponding ratios from rat tail tendon, calculated from Wess et al. [21].

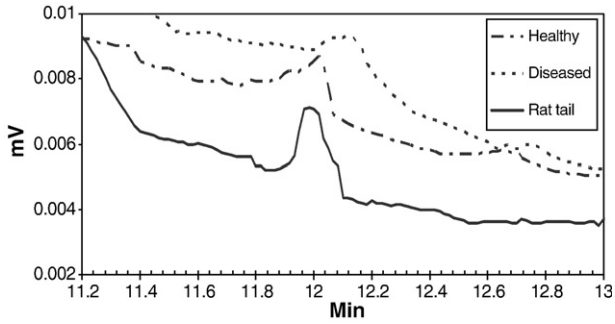

Fig. 3. The diagram shows a typical chromatogram of mature pyridinoline cross-links. From top to bottom: diseased leaflet, healthy (grossly uninvolved) leaflet, and rat tail.

3.4. High-performance liquid chromatography

A series of different runs were completed using various concentrations of standard mature cross-link in order to characterize the exact appearance of the related peaks in the chromatogram and secondly to produce a standard graph. Fig. 3 shows a typical chromatogram of mature cross-links. Taking into account the pattern of the chromatogram of amino acids, we conducted another series of HPLC runs using standard amino acids in order to calibrate the machine and also to see whether there would be any possible peak interference with those of standard mature cross-links. It is apparent from the figure that, in all runs, only one type of mature cross-link, namely, pyridinoline, was detectable in

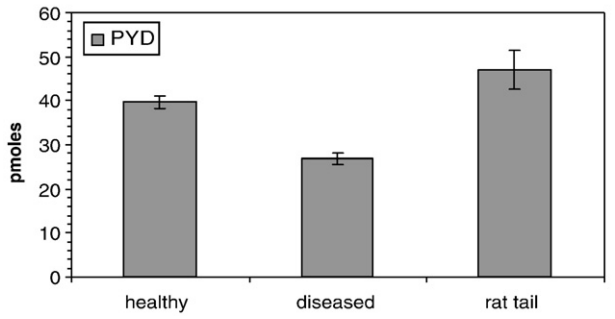

Fig. 4. The figure shows the amount of the pyridinoline cross-links in 20 μg of collagen sample. The error bars are derived from standard deviation and for healthy (grossly uninvolved), diseased, and rat tail are 1.53, 1.16, and 4.37 pmol, respectively.

the rat tail and valve samples irrespective of their disease status. The analytical areas for the respective peaks were determined, and the concentration of pyridinoline was calculated in terms of picomoles. Statistical analysis was carried out using Kruskal–Wallis for analysis of variance ($P \leq .05$). Fig. 4 shows the amount of the pyridinoline cross-links in the respective samples. It can be seen that the amount of mature cross-link, pyridinoline, in healthy leaflets is significantly greater than that in diseased leaflets.

3.5. Reanalysis of X-ray data

In order to compare the new data from this study with results already published by the authors, a reanalysis was performed on X-ray diffraction data from a study that mapped collagen fibrils and its quantitative and qualitative values in affected and the adjacent grossly uninvolved areas of (MMVD) leaflets [10]. The reanalysis was performed on the summed meridional diffraction intensities; normalized using readings taken from ion chambers placed before and after the sample. This produced a value that is proportional to the collagen fibril content per unit mass of tissue. The results of reanalysis of X-ray data confirmed a 20% decrease in intact collagen fibrils in the diseased areas ($P \leq .05$). It should be noted that this diffraction technique reports the relative amounts of diffracting structure (i.e., collagen fibrils) and does not take into account the presence of nonfibrillar collagen.

4. Discussion

This study demonstrated a 10% reduction in total collagen and a 20% reduction in fibrillar collagen content in the myxomatous areas of canine valves with mild to moderate disease. Furthermore, there is an increase in immature reducible covalent cross-links in diseased areas, while the amount of nonreducible mature cross-links has declined in the same diseased leaflets. Cross-links contribute to collagen mechanical strength, and a combination of collagen loss, failure to form collagen fibrils, and abnormal cross-linkages would all contribute to reduced mechanical strength. The potential confounding factor that these changes might be a natural age-dependent alteration in collagen expression was overcome by comparing diseased and the adjacent grossly uninvolved areas within the same leaflet. Considering the close age association with MMVD, this is important as it suggests a true disease-associated dyscollagenesis rather than an age-related change.

Previous reports on collagen changes in MMVD in both dogs and humans have been incomplete, mainly descriptive, or even contradictory [4,6–9]. We have previously demonstrated reduction in total collagen content and alteration in collagen alignment and how these changes are located to a narrow distal zone at the valve edge [10]. Furthermore, we have shown that such changes can be patchy in distribution and this understanding of the local and regional alteration in collagen deposition, collagen alignment, and collagen maturation has significantly improved our understanding of disease pathogenesis. The data presented here are only for mild to moderately affected leaflets, and the extent of further change in severe forms of the disease cannot be determined from the present study. However, we have demonstrated that distinct changes are already apparent in the early stages of this disease, which can be presumed to contribute to abnormalities of mechanical function of the mitral valve complex.

Measurements of the melting process by DSC give insight into the structural alteration that occurs with myxomatous degeneration. The thermal stability of collagen depends on the level of hydration of collagen and the number and the nature of covalent cross-links [27,28]. The mechanism of denaturation is based on an irreversible process beginning with the rupture of hydrogen bonds uncoupling the three α-chains followed by breakage of the cross-link bonds [29,30]. In the presence of thermally stable cross-links, dehydration may have a role in this process by reducing the free volume available for denaturation of α-chains in the collagen fibers [31]. Furthermore, dehydrated collagen would be confined in a spatial arrangement within the lattice of the fiber, decreasing the entropy and subsequently raising the thermal stability of collagen (polymer-in-a-box theory). An alternative explanation is that, with fiber dehydration, water molecules that are connected via hydrogen bonds to the triple helix itself would be gradually stripped away. Some of these molecules are involved in water bridge structures that connect one α-chain to another. These hydrogen bonds would need to be broken on denaturation. The stripping away of water bridge molecules means fewer hydrogen bonds need to be broken to separate and uncouple the α-chains and reduce collagen to random coils. At an ultrastructural level, this collagen disorganization can be seen in dog mitral valves on transmission electron microscopy [9].

Although the enthalpy of denaturation was decreased by 20% in diseased valve tissue, this effect cannot simply be due to collagen depletion as the hydroxyproline assay only identified a 10% decrease in collagen. Together these findings demonstrate qualitative and quantitative changes in valve collagen. There was no significant difference in the onset temperature of denaturation comparing diseased and the adjacent grossly uninvolved tissue samples. It is already known that a change in pH or concentration of ions around the collagen molecules only influences the temperature but not the enthalpy of denaturation [32], and it is likely that changes in amino acid composition have a similar effect. The most likely explanation for this diminished enthalpy is that not all of the collagen molecules are in the form of intact and regularly structured triple helices and/or fibrils. This was confirmed by a reanalysis of data from our previous X-ray diffraction study. Only the regularly ordered and intact fibrils could contribute to the diffraction pattern, and by comparing affected and grossly uninvolved leaflets there is a clear 20% decrease in intact collagen fibrils. This nonfibrillous collagen

could arise from failure of incorporation of the molecules in fibrils, uncoupling of the α-chains as a result of enzymatic depolymerization and subsequent denaturation, and, finally, an alteration in the nature and number of the cross-links responsible for strengthening the collagen helices. Overall, these factors would not affect the onset temperature of denaturation, but the enthalpy would undergo some changes. This would be consistent with the findings of a previous study carried out on the superficial digital flexor tendon degeneration in horses which showed that the enthalpy of denaturation of degenerated tendon was less than that of normal tendon, whereas the temperature characteristics were the same [32]. Interestingly, both these diseases appear in advanced age and both have been suggested to be associated with a repeated injury mechanism.

The neutron diffraction data from dog tail showed the systematic changes that are comparable to those reported by Wess et al. [21,22], indicating the presence of a high number of reducible cross-links in the tendon tail. The mitral valve results showed a marked difference in the number of reducible cross-links compared to tail tendon irrespective of pathological status. However, according to the same set of neutron data, there was a higher level of reducible cross-links in the diseased leaflet. Complementing this data, HPLC showed that the amounts of nonreducible mature cross-links were higher in healthy leaflets. Cross-links are formed through the intermolecular reactions of aldehyde residues catalyzed by lysyl oxidase. Initially, there are two pathways based on the precursor, namely, lysine aldehyde and hydroxylysine aldehyde. The latter is the predominant form in most connective tissues. Both of these pathways lead to the production of cross-links which are primary borohydride reducible giving the opportunity to be investigated by neutron diffraction. During the course of maturation of the fibrils, these reducible cross-links tend to be replaced by mature nonreducible cross-links [33]. Pyridinoline and deoxypyridinoline have been identified so far as two important mature nonreducible cross-links, with deoxypyridinoline almost exclusively associated with bone tissue. The cross-links are a major contributor to the expected strength and mechanical properties of collagen.

The observed changes in the amount of cross-links can be interpreted in a variety of ways. Studies of other systems have shown that, with the advancing of age and as MMVD is an age-related disease, the activity of lysyl oxidase decreases. This means that, in general, older tissues will tend to have fewer cross-links [33]. Increased deposition of proteoglycans, which is recognized to occur with MMVD, might interfere with the formation of cross-links [34]. Lastly, accumulation of advanced glycation end products (AGEs), which are nonenzymatic cross-links derived from prolonged exposure to monosaccharides, has also been reported to have detrimental effects on the mechanical properties of connective tissues and might also interfere with the formation of enzymatic cross-links. There is increasing interest in the role of AGEs in the process of aging [35,36]. However, in the current study, the alteration in cross-links could be explained in terms of dyscollagenesis associated with myofibroblasts activation [10,11]. The products of activated myofibroblasts would be immature collagen molecules, and as turnover increases there may not be enough time for the transformation of immature reducible cross-links to the mature ones. The reduction in tensile strength of the leaflets could further contribute to mitral valve prolapse and leaflet extensibility, both of which are features of MMVD in dogs and MVP in humans [37,38]. This in itself could contribute to ongoing and progressive pathological changes to the leaflets.

In conclusion, this study has demonstrated changes in fibrillar collagen, total collagen content, and collagen cross-links in mild to moderate MMVD in the dog and provides evidence that the pathology of this disease involves a process of dyscollagenesis. These findings have implications for understanding the natural progression of this disease both in dogs and in humans.

Acknowledgments

The authors would like to thank the following people for their technical support: Graham Pettigrew, Demé Bruno, Farid Sa'Adedin, Yan C.S.M. Laurenson, and Lijing Ke.

References

[1] Beardow AW, Buchanan JW. Chronic mitral valve disease in Cavalier King Charles Spaniels: 95 cases (1987–1991). J Am Vet Med Assoc 1993;203(7):1023–9.
[2] Buchanan JW. Chronic valvular disease (endocardiosis) in dogs. Adv Vet Sci Comp Med 1977;21:75–106.
[3] Pederson HD, Haggstrom J. Mitral valve prolapse in the dog: a model of mitral valve prolapse in man. Cardiovasc Res 2000;47(2):234–43.
[4] Fornes P, Heudes D, Fuzellier JF, Tixier D, Bruneval P, Carpentier A. Correlation between clinical and histologic patterns of degenerative mitral valve insufficiency: a histomorphometric study of 130 excised segments. Cardiovasc Pathol 1999;8:81–92.
[5] Kogure K. Pathology of chronic mitral valvular disease in the dog. Nippon Juigaku Zasshi 1980;42:323–35.
[6] Tamura K, Fukuda Y, Ishizaki M, Masuda Y, Yamanaka N, Ferrans VJ. Abnormalities in elastic fibers and other connective-tissue components of floppy mitral valve. Am Heart J 1995;129:1149–58.
[7] Henney AM, Parker DJ, Davies MJ. Collagen biosynthesis in normal and abnormal human heart valves. Cardiovasc Res 1982;16:624–30.
[8] Henney AM, Tsipouras P, Schwartz RC, Child AH, Devereux RB, Leech GJ. Genetic evidence that mutations in the COL1A1, COL1A2, COL3A1, or COL5A2 collagen genes are not responsible for mitral valve prolapse. Br Heart J 1989;61:292–9.
[9] Black A, French AT, Dukes-McEwan J, Corcoran BM. Ultrastructural morphologic evaluation of the phenotype of valvular interstitial cells in dogs with myxomatous degeneration of the mitral valve. Am J Vet Res 2005;66(8):1408–14.
[10] Hadian M, Corcoran BM, Han RI, Grossmann JG, Bradshaw JP. Collagen organisation in canine myxomatous mitral valve disease, an x-ray diffraction study. Biophys J 2007;93(7):2472–6.
[11] Disatian S, Ehrhart EJ, Zimmerman S, Orton EC. Interstitial cells from dogs with naturally occurring myxomatous mitral valve disease undergo phenotype transformation. J Heart Valve Dis 2008;17:402–11.
[12] Han RI, Black A, Culshaw GJ, French AT, Else RW, Corcoran BM. Distribution of myofibroblasts, smooth muscle-like cells, macro-

phages, and mast cells in mitral valve leaflets of dogs with myxomatous mitral valve disease. Am J Vet Res 2008;69:763–9.
[13] Rabkin E, Aikawa M, Stone JR, Fukumoto Y, Libby P, Schoen FJ. Activated interstitial myofibroblasts express catabolic enzymes and mediate matrix remodelling in myxomatous heart valves. Circulation 2001;104(21):2525–32.
[14] Soini Y, Satta J, Maatta M, Autio-Harmainen H. Expression of MMP2, MMP9, MT1-MMP, TIMP1, and TIMP2 mRNA in valvular lesions of the heart. J Pathol 2001;194:225–31.
[15] Robins SP, Bailey AJ. The chemistry of the collagen cross-links. Biochem J 1977;163:339–46.
[16] Silver FH, Freeman JW, Seehra GP. Collagen self-assembly and the development of tendon mechanical properties. J Biomech 2003;36: 1529–53.
[17] Misof K, Landis WJ, Klaushofer K, Frazl P. Collagen from the osteogenesis imperfecta mouse model (oim) shows reduced resistance against tensile stress. J Clin Invest 1997;100:40–5.
[18] Whitney JC. Observations on the effect of age on the severity of heart valve lesions in the dog. J Small Anim Pract 1974;15(8):511–22.
[19] Kafienah W, Buttle DJ, Burnett D, Hollander AP. Cleavage of native type I collagen by human neutrophil elastase. Biochem J 1998;1: 897–902.
[20] Hurtig M, Pearce S, Warren S, Kalra M, Mirzaie M. Arthroscopic mosaic arthroplasty in the equine third carpal bone. Vet Surg 2001;30: 228–39.
[21] Wess TJ, Wess L, Miller A, Lindsay RM, Baird JD. The in vivo glycation of diabetic tendon collagen studied by neutron diffraction. J Mol Biol 1993;230:1297–303.
[22] Wess TJ, Miller A, Bradshaw JP. Cross-linkage sites in type I collagen fibrils studied by neutron diffraction. J Mol Biol 1990;213:1–5.
[23] Bartolomeo MP, Maisano F. Validation of a reversed-phase HPLC method for quantitative amino acid analysis. J Biomol Tech 2006;17 (2):131–7.
[24] Jarrett HW, Cooksy KD, Ellis B, Anderson JM. The separation of *o*-phthalaldehyde derivatives of amino acids by reversed-phase chromatography on octylsilica columns. Anal Biochem 1986;153(1): 189–98.
[25] O'Leary R, Rerek M, Wood EJ. Fucoidan modulates the effect of transforming growth factor (TGF)-beta1 on fibroblast proliferation and wound repopulation in in-vitro models of dermal wound repair. Biol Pharm Bull 2004;27(2):266–70.
[26] Collier RJ, Stiening CM, Pollard BC, VanBaale MJ, Baumgard LH, Gentry PC, Coussens PM. Use of gene expression microarrays for evaluating environmental stress tolerance at the cellular level in cattle. J Anim Sci 2006;84(Suppl):E1–E13.
[27] Sionkowska A. Thermal denaturation of UV-irradiated wet rat tail tendon collagen. Int J Biol Macromol 2005;35:145–9.
[28] Trebacz H, Wójtowicz K. Thermal stabilization of collagen molecules in bone tissue. Int J Biol Macromol 2005;37:257–62.
[29] Miles CA. Kinetics of collagen denaturation in mammalian lens capsules studied by differential scanning calorimetry. Int J Biol Macromol 1993;15:265–71.
[30] Miles CA, Burjanadze TV, Bailey AJ. The kinetics of the thermal denaturation of collagen in unrestrained rat tail tendon determined by differential scanning calorimetry. J Mol Biol 1995;245:437–46.
[31] Miles CA, Ghelashvili M. Polymer-in-a-box mechanism for the thermal stabilization of collagen molecules in fibers. Biophys J 1999;76:3243–52.
[32] Miles CA, Wardale RJ, Brich HL, Bailey AJ. Differential scanning calorimetric studies of superficial digital flexor tendon degeneration in the horse. Equine Vet J 1994;26:291–6.
[33] Eyre DR, Dickson IR, Van Ness K. Collagen cross-linking in human bone and articular cartilage. Age-related changes in the content of mature hydroxypyridinium residues. Biochem J 1988;252:495–500.
[34] Scott JE, Orford CR. Dermatan sulphate-rich proteoglycan associates with rat tail-tendon collagen at the d band in the gap region. Biochem J 1981;197:213–6.
[35] Haus JM, Carrithers JA, Trappe SW, Trappe TA. Collagen, cross-linking, and advanced glycation end products in aging human skeletal muscle. J Appl Physiol 2007;103(6):2068–76.
[36] Shiraki M, Kuroda T, Tanaka S, Saito M, Fukunaga M, Nakamura T. Nonenzymatic collagen cross-links induced by glycoxidation (pentosidine) predicts vertebral fractures. J Bone Miner Metab 2008;26(1): 93–100.
[37] Hayek E, Gring CN, Griffin BP. Mitral valve prolapse. Lancet 2005; 365:507–18.
[38] Hyun C. Mitral valve prolapse in Cavalier King Charles Spaniel: a review and case study. J Vet Sci 2005;6:67–73.